Pre- and Postinvasion Defenses Both Contribute to Nonhost Resistance in Arabidopsis

Volker Lipka, *et al.*

Science **310**, 1180 (2005);
DOI: 10.1126/science.1119409

the Intertrappean beds of India makes it plausible that hypsodonty in these animals was an adaptation to feeding on abrasive grasses. Moreover, the phytolith data suggest that silica production in grasses comparable with that observed in extant taxa appeared to have evolved by the Late Cretaceous. This rejects the view that modern levels of phytolith production were an evolutionary response to grazing during the Cenozoic (*28*) and suggests that the high silica levels of grasses are the result of coevolution with Late Cretaceous herbivores (such as gondwanatherians or insects) or of a process unrelated to plant/herbivore interaction.

References and Notes

1. Grass Phylogeny Working Group, *Ann. Mo. Bot. Gard.* **88**, 373 (2001).
2. B. F. Jacobs, J. D. Kingston, L. L. Jacobs, *Ann. Mo. Bot. Gard.* **86**, 590 (1999).
3. K. Bremer, *Evolution* **56**, 1374 (2002).
4. C. A. E. Strömberg, *Proc. Natl. Acad. Sci. U.S.A.* **102**, 11980 (2005).
5. T. Janssen, K. Bremer, *Bot. J. Linn. Soc.* **146**, 385 (2004).
6. P. M. Barrett, K. J. Willis, *Biol. Rev. Camb. Philos. Soc.* **76**, 411 (2001).
7. J. A. Wilson, P. C. Sereno, *Mem. Soc. Vertebr. Paleontol.* **5**, 1 (1998).
8. D. W. Krause, G. V. R. Prasad, W. von Koenigswald, A. Sahni, F. E. Grine, *Nature* **390**, 504 (1997).
9. D. W. Krause, M. D. Gottfried, P. M. O'Connor, E. M. Roberts, *Acta Palaeontol. Pol.* **48**, 321 (2003).
10. R. S. Rana, G. P. Wilson, *Acta Palaeontol. Pol.* **48**, 331 (2003).
11. R. Patnaik, A. Sahni, G. V. R. Prasad, *J. Palaeontol. Soc. India* **46**, 15 (2001).
12. C. A. Matley, *Rec. Geol. Surv. India* **74**, 535 (1939).
13. F. B. Von Huene, C. A. Matley, *Mem. Geol. Surv. India* **21**, 1 (1933).
14. P. Ghosh *et al.*, *Cretaceous Res.* **24**, 743 (2003).
15. N. Sharma, R. K. Kar, A. Agarwal, R. Kar, *Micropaleontology* **51**, 73 (2005).
16. Materials and methods are available as supporting material on *Science* Online.
17. C. A. E. Strömberg, *Palaeogeogr. Palaeoclimatol. Palaeoecol.* **207**, 239 (2004).
18. S. D. Chitaley, M. T. Sheikh, *J. Indian Bot. Soc.* **50**, 137 (1971).
19. G. V. Patil, R. B. Singh, *A. K. Ghosh Commemoration Volume*, A. K. Sharma, G. C. Mitra, M. Banerjee, Eds. (Today and Tomorrow's Printers & Publishers, New Delhi, India, 1984), pp. 89–96.
20. B. S. Trivedi, S. K. Bajpai, *J. Indian Bot. Soc.* **61**, 320 (1982).
21. B. Samant, D. M. Mohabey, paper presented at the XIX Indian Colloquium on Micropalaeontology and Stratigraphy, Symposium on Recent Developments in Indian Ocean Palaeoceanography and Palaeoclimate, Varanasi, India, 9 to 11 October 2003.
22. S. McLoughlin, *Aust. J. Bot.* **49**, 271 (2001).
23. W. C. Clyde, I. H. Khan, P. D. Gingerich, *Geology* **31**, 1097 (2003).
24. W. W. Hay *et al.*, in *Evolution of the Cretaceous Ocean–Climate System*, E. Barrera, C. C. Johnson, Eds. (Geological Society of America, Boulder, CO, 1999), pp. 1–47.
25. J. A. Case, *J. Vertebr. Paleontol.* **22**, 42A (2002).
26. K. Chin, B. D. Gill, *Palaios* **11**, 280 (1996).
27. R. A. Rodríguez de la Rosa, S. R. S. Cevallos-Ferriz, A. Silva-Pineda, *Palaeogeogr. Palaeoclimatol. Palaeoecol.* **142**, 231 (1998).
28. G. L. Stebbins, *Ann. Mo. Bot. Gard.* **68**, 75 (1981).
29. V. Courtillot *et al.*, *Nature* **333**, 843 (1988).
30. C. K. Khajuria, G. V. R. Prasad, B. K. Manhas, *Newsl. Stratigr.* **31**, 21 (1994).
31. M. Widdowson, M. S. Pringle, O. A. Fernandez, *J. Petrol.* **41**, 1177 (2000).

32. We thank N. C. Mehrotra for facilities and support, and S. Kad and K. Ambwani for help. C.A.E.S. is supported by a grant to E. M. Friis and L. Werdelin at the Swedish Museum of Natural History, Stockholm. We thank J. A. Wilson, G. P. Wilson, and two anonymous reviewers for helpful comments and suggestions.

Supporting Online Material

www.sciencemag.org/cgi/content/full/310/5751/1177/DC1
Materials and Methods
SOM Text
Fig. S1
Table S1
References

12 August 2005; accepted 12 October 2005
10.1126/science.1118806

Pre- and Postinvasion Defenses Both Contribute to Nonhost Resistance in *Arabidopsis*

Volker Lipka,[1]*† Jan Dittgen,[1]* Pawel Bednarek,[1] Riyaz Bhat,[1] Marcel Wiermer,[1] Monica Stein,[2] Jörn Landtag,[3] Wolfgang Brandt,[4] Sabine Rosahl,[3] Dierk Scheel,[3] Francisco Llorente,[5] Antonio Molina,[5] Jane Parker,[1] Shauna Somerville,[2] Paul Schulze-Lefert[1]‡

Nonhost resistance describes the immunity of an entire plant species against nonadapted pathogen species. We report that *Arabidopsis* PEN2 restricts pathogen entry of two ascomycete powdery mildew fungi that in nature colonize grass and pea species. The PEN2 glycosyl hydrolase localizes to peroxisomes and acts as a component of an inducible preinvasion resistance mechanism. Postinvasion fungal growth is blocked by a separate resistance layer requiring the EDS1-PAD4-SAG101 signaling complex, which is known to function in basal and resistance (*R*) gene–triggered immunity. Concurrent impairment of pre- and postinvasion resistance renders *Arabidopsis* a host for both nonadapted fungi.

Host cell entry represents a critical step during pathogenesis of invasive animal and plant parasites (*1*, *2*). This is usually not a barrier to adapted phytopathogenic fungi that are able to infect a plant species. However, in plant species beyond the host range of a pathogen, called nonhost plants, parasitic fungi typically fail to enter attacked plant cells (*3*, *4*). In the nonhost interaction between *Arabidopsis* and the grass powdery mildew fungus, *Blumeria graminis* f. sp. *hordei* (*Bgh*), three *Arabidopsis pen* (penetration) mutant loci were recovered that permit, at high frequency, entry of the nonadapted parasite (*5*), thereby providing initial evidence for the existence of a plant-controlled process terminating fungal ingress at the cell periphery. *AtPEN1* encodes a soluble NSF (*N*-ethylmaleimide–sensitive factor) attachment protein receptor (SNARE)–domain-containing and plasma-membrane resident syntaxin, which becomes recruited into plasma membrane microdomains beneath incipient fungal entry sites (*6*, *7*). Because SNARE proteins play a key role in vesicle trafficking in eukaryotic cells (*8*), these findings have been interpreted as evidence for the existence of a vesicle-associated resistance mechanism preventing powdery mildew ingress.

Although each of the isolated *pen* mutants (*pen1*, *pen2*, and *pen3*) permits efficient *Bgh* entry, initiation of postinvasive fungal growth invariably ceases, and this coincides with a cell death response of epidermal cells with haustorial complexes (*5*). We performed a time-course experiment and compared *Bgh* entry rates in wild type, *pen1*-1, *pen2*-1, and *pen1 pen2* double null mutants (Fig. 1). Entry rates were seven- and fivefold higher than wild type in *pen1* and *pen2* mutants, respectively. An 11-fold increase over wild type was seen in the *pen1 pen2* genotype, suggesting *PEN1* and *PEN2* act in separate defense pathways (Fig. 1). Elevated fungal entry rates were associated with an increased incidence of invasion-associated cell death (Fig. 1). To assess the importance of *PEN1* and *PEN2* functions in a further powdery mildew nonhost interaction, we examined the mutant *Arabidopsis* genotypes with *Erysiphe pisi*, which colonizes dicotyledonous pea plants in nature. Like *Bgh*, *E. pisi* fails to reproduce on *Arabidopsis* but

[1]Department of Plant Microbe Interactions, Max Planck Institute for Plant Breeding Research, Carl von Linné Weg 10, D-50829 Köln, Germany. [2]Department of Plant Biology, Carnegie Institute of Washington, Stanford, CA 94305, USA. [3]Department of Stress and Developmental Biology, [4]Department of Bioorganic Chemistry, Institute of Plant Biochemistry, Weinberg 3, D-06120 Halle (Saale), Germany. [5]Laboratorio de Bioquímica y Biología Molecular, Departamento de Biotecnología-Universidad Politécnica de Madrid Escuela Técnica Superior de Ingenieros Agrónomos, Avenida Complutense s/n, E-28040 Madrid, Spain.

*These authors contributed equally to this work.
†Present address: Zentrum für Molecularbiologie der Pflazen, Plant Biochemistry, Eberhard-Karls-Universität Tübingen, Auf der Morgenstelle 5, D-72076 Tübingen, Germany.
‡To whom correspondence should be addressed. E-mail: schlef@mpiz-koeln.mpg.de

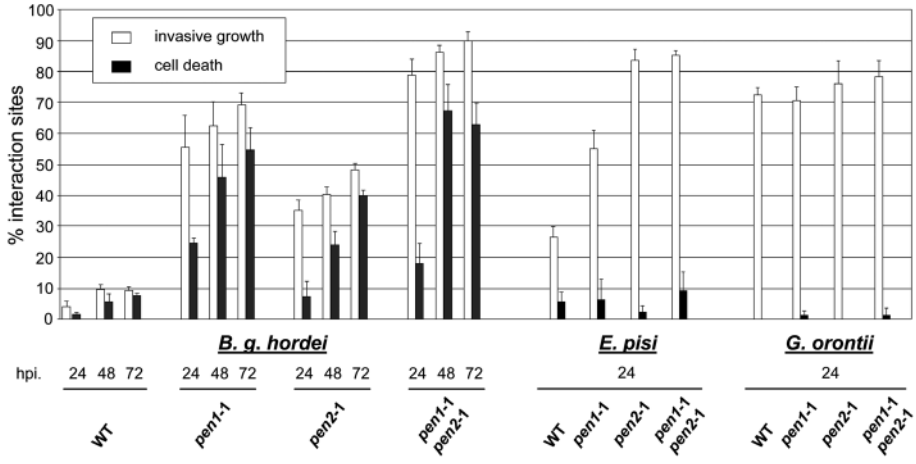

Fig. 1. Frequency of invasive growth and epidermal single-cell death at *B. g. hordei*, *E. pisi*, and *G. orontii* interaction sites on *Arabidopsis* wild type (WT) and *pen1*-1, *pen2*-1 and *pen1*-1 *pen2*-1 mutants. hpi, hours post–conidiospore inoculation. Error bars indicate standard deviations for triplicate measurements.

is phylogenetically more closely related to the *Arabidopsis*-infecting powdery mildew *E. cruciferarum* than to *Bgh* (*9*). Absence of PEN1 or PEN2 greatly enhanced the entry rates of *E. pisi*. However, *E. pisi* successfully invaded wild-type *Arabidopsis* more often than *Bgh* [~25% versus ~5% at 24 hours postinoculation (Fig. 1)], and lack of PEN2 alone permitted an *E. pisi* entry frequency similar to those of the *pen1 pen2* double mutants (Fig. 1). Invasiveness of *Bgh* on *pen1 pen2* double mutants and of *E. pisi* on *pen2* or *pen1 pen2* plants is essentially indistinguishable from that of the adapted *Golovinomyces orontii* powdery mildew on wild-type *Arabidopsis* (70 to 80%) (Fig. 1). Invasiveness of *G. orontii* does not increase on either *pen* mutant genotype, indicating that PEN1 and PEN2 exert entry-limiting functions only in nonhost powdery mildew interactions.

A difference between *pen1* and *pen2* plants was revealed after inoculation with the nonadapted hemibiotrophic oomycete *Phytophthora infestans*. Only *pen2* mutants allowed frequent initiation of invasive growth of this potato pathogen (fig. S1A). Similar to invasion-associated cell death in interactions with the inappropriate powdery mildew species (Fig. 1 and fig. S1B), invasive growth of the oomycete in *pen2* plants is linked to a localized plant cell death response (fig. S1C). Likewise, inoculation with the broad host range ascomycete *Plectosphaerella cucumerina* resulted in enhanced disease susceptibility only in *pen2* mutants (fig. S1D). Thus, PEN2 limits growth of a wide spectrum of pathogens, whereas PEN1 function is limited to nonadapted powdery mildew species.

PEN2 was isolated by map-based cloning (fig. S2A) and encodes 1 out of 48 predicted *Arabidopsis* family 1 glycosyl hydrolases (F1GHs) (fig. S2B). Both chemically induced *pen2* mutant alleles, *pen2*-1 and *pen2*-3, are characterized by point mutations, each generating stop codons that lead to truncated peptides (fig. S2, B and C). We also isolated a homozygous transfer DNA (T-DNA) insertion line resulting in loss of detectable PEN2 transcript and protein (designated *pen2*-2; fig. S2, A to C). The infection phenotype of *pen2*-2 plants is indistinguishable from the two chemically induced mutants. F1GHs are present in all eukaryotic and prokaryotic organisms and hydrolyze O or S glycosidic bonds between two or more carbohydrates or between a carbohydrate and a noncarbohydrate (i.e., aglycone). In plants, F1GHs have been implicated in a wide range of processes, including development, cell wall modification, and chemical defense against pathogens (*10*).

Cyanogenic β-glucosidase CBG1 from *Trifolium repens* shares 48% sequence identity (65% similarity) with PEN2 (fig. S2B). This enabled us to use the known three-dimensional structure of CBG1 as template for homology modeling of a PEN2 structure (Fig. 2A and Materials and Methods). The topview ribbon diagram of PEN2 shows the typical F1GH barrel fold structure with a central cleft gate to the active site, which harbors the catalytic machinery consisting of two conserved acid/base and nucleophilic glutamates (Glu^{183} and Glu^{398}, denoted by E183 and E398, respectively), located at the bottom of the active site pocket (Fig. 2A) (*11*). To test whether PEN2 catalytic activity is required for pathogen entry control, we generated transgenic lines in a *pen2*-1 mutant background, expressing a $Glu^{183} \rightarrow Asp^{183}$ (E183D) substitution variant of PEN2 ($PEN2_{E183D}$) under the control of native *PEN2* 5′ regulatory sequences (fig. S2D). Unlike control transgenic lines expressing wild-type PEN2, none of the tested $PEN2_{E183D}$ lines complemented the *pen2* mutant phenotype, although a PEN2-specific antiserum detected comparable $PEN2_{E183D}$ protein amounts in leaf extracts (Fig. 2B). This suggests that PEN2 catalytic activity is required to restrict pathogen entry.

An unusual feature of the PEN2 F1GH is the presence of a C-terminal extension containing a low-complexity region of 15 amino acids followed by a predicted helical region of 28 amino acids (Fig. 2A and fig. S2B). To test a potential functional contribution of the C-terminal extension, we generated transgenic lines in the *pen2*-1 background expressing a truncated PEN2 protein that lacked the C-terminal 28 amino acids ($PEN2_{\Delta 28}$; fig. S2, B and D). Although the truncation did not affect protein stability (Fig. 2B), $PEN2_{\Delta 28}$ failed to complement the *pen2* phenotype upon *Bgh* or *E. pisi* challenge, indicating that the C-terminal extension may regulate enzyme activity and/or serve as a determinant for subcellular localization.

To examine PEN2 localization in living cells, we generated transgenic lines expressing various PEN2–green fluorescent protein (GFP) fusion constructs driven by native 5′ regulatory *PEN2* sequences in the *pen2*-1 null mutant background. Because both N- and C-terminal fusions of PEN2 to GFP were found to produce nonfunctional proteins, we searched for candidate GFP insertion sites in PEN2 on the basis of the deduced structural model (Fig. 2A). Indeed, insertion of GFP between the predicted globular PEN2 enzyme and the C-terminal extension resulted in a fluorescent fusion protein that complemented the *pen2* phenotype. Confocal imaging revealed a distinctive subcellular GFP fluorescence pattern, indicating association of PEN2 to mobile vesicle-like bodies (Fig. 2C). Coexpression of fluorophore-tagged marker proteins for the Golgi, mitochondria, or peroxisomes identified these as peroxisomes in time-lapse imaging experiments (fig. S3A), which is in agreement with the PEN2 subcellular localization predicted by PSORT (*12*). The two-color imaging experiments showed the expected matrix localization for red fluorescent protein (RFP) containing a type 1 peroxisomal targeting sequence, whereas PEN2-GFP appeared to be confined to the periphery of peroxisomes (fig. S3A). A striking focal accumulation of PEN2-GFP-tagged peroxisomes was seen upon inoculation with *Bgh* conidiospores at incipient entry sites (14 to 16 hours postinoculation) (Fig. 2D). This pathogen-inducible PEN2 accumulation at fungal entry sites coincides with its predicted biological function at the cell periphery and is distinct from the recruitment of PEN1 syntaxin in a plasma membrane microdomain beneath fungal appressoria (*6*, *7*). Independent biochemical fractionation of crude leaf protein extracts in soluble and microbody membrane fractions corroborated an association of wild-type PEN2 with microbody membrane fractions and revealed only trace amounts in enriched plasma membrane vesicles (fig. S3B). A substantial PEN2 portion was also found in corresponding soluble fractions, possibly due to a partial dissociation

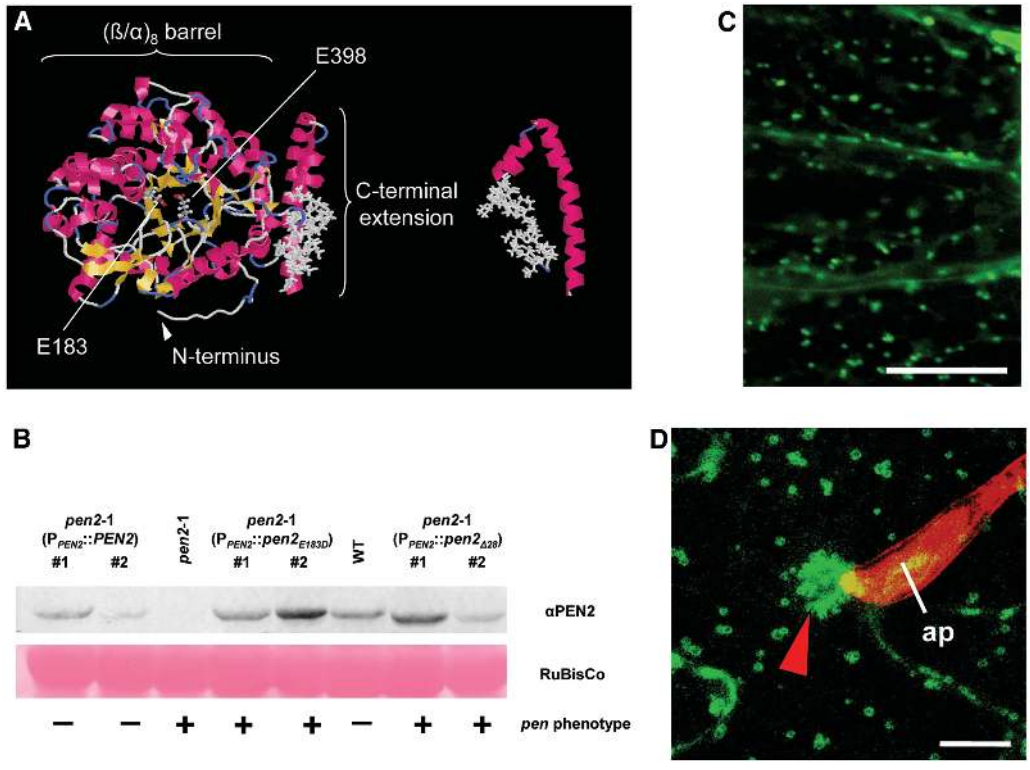

Fig. 2. Analysis of PEN2 function and subcellular localization. (**A**) Topview ribbon diagram of a PEN2 structure model. The catalytic machinery consists of two conserved acid/base and nucleophilic glutamates (E183 and E398). The unique C-terminal extension (90° rotated view shown separately on the right) includes a low complexity region (white ball and stick presentation) followed by a predicted helical region of 28 amino acids. (**B**) Immunodetection of PEN2 in crude leaf protein extracts using a PEN2 antibody. PEN2 accumulation in independent transgenic lines (labeled 1 and 2) expressing wild-type *PEN2* or catalytically inactive ($pen2_{E183D}$) or C-terminally truncated ($pen2_{\Delta 28}$) versions driven by native 5′ regulatory sequences (P_{PEN2}). Complementation of the *pen2* phenotype after *Bgh* inoculation experiments is denoted by + or – below each lane. Ponceau S detection of RuBisCo was used as protein loading control. (**C**) Confocal laser scanning microscopy of leaf epidermal cells in transgenic *pen2*-1 mutants expressing a functional PEN2-GFP fusion reveals association with vesicle-like bodies. Scale bar, 10 μm. (**D**) Peroxisomes containing PEN2-GFP accumulate at *Bgh* entry sites (marked by red arrowhead). Fungal structures are stained in red color by propidium iodide. Scale bar, 10 μm. ap, appressorium.

from peroxisomal membranes during the fractionation procedure.

Although the identified *pen* single mutants (*pen1*, *pen2*, and *pen3*) or the double mutant *pen1 pen2* compromise nonhost resistance at the cell periphery, each mutant line retains the ability to mount effective postinvasion immunity, which is linked to a cell death response (Fig. 1 and fig. S1B). Sustained postentry growth of powdery mildews requires a haustorial complex in living epidermal cells to supply nutrients for hyphal growth on the leaf surface (epiphytic hyphae). The lipase-like EDS1 protein and its sequence-related interaction partners PAD4 and SAG101 are known to play a critical role in a subset of R protein–triggered and basal immune responses to invasive biotrophic pathogens (*13*). *Bgh* entry rates on single *eds1*, *pad4*, and *sag101* mutants were not significantly different from those found in wild type. Although interaction sites containing haustorial complexes showed an increased incidence of epiphytic fungal growth on each of these mutants relative to wild type, colonization attempts usually ceased after the formation of two to three elongating hyphae. However, we noted that about 2% of such sites on *pad4* and *eds1* plants permitted sustained epiphytic hyphal growth (i.e., microcolony formation) (Fig. 3A). Although the incidence of epiphytic fungal growth was further enhanced upon introgression of the *pen2* null mutation in the single mutants (forming *pen2 sag101*, *pen2 pad4*, and *pen2 eds1* double mutants), the frequency of microcolony formation remained low (Fig. 3A). Because the function of PAD4 and SAG101 in basal and R protein–triggered immunity were recently found to be partially redundant (*13*), we also challenged *pad4 sag101* double mutants with *Bgh*. Although pathogen entry rates on *pad4 sag101* lines were indistinguishable from that of wild type, microcolony formation was enhanced relative to those of the single mutants, suggesting similarly redundant activities of sequence-related PAD4 and SAG101 proteins in nonhost resistance (Fig. 3A). The incidence of microcolony formation was further increased in *pen2 pad4 sag101* triple mutants, revealing synergistic interactions between PEN2 and the redundant functions of PAD4 and SAG101 (Fig. 3A). We occasionally found conidiophores containing mature conidiospores on microcolonies of *pen2 pad4 sag101* leaves, indicating breakdown of nonhost resistance to the grass powdery mildew fungus (fig. S3D).

In interactions with *E. pisi*, entry rates of single *eds1*, *pad4*, and *sag101* mutants were not altered relative to those of wild-type plants, whereas epiphytic hyphal growth increased substantially on the former two mutant lines (fig. S3C). A synergistic effect was seen after introgression of *pen2* in *eds1* or *pad4* backgrounds (*pen2 eds1* and *pen2 pad4* plants), indicating separable functions for and synergistic activities of the respective wild-type genes in pre- and postinvasion resistance. Although sporulation was not detectable on the single mutants, both *pen2 eds1* and *pen2 pad4* plants supported *E. pisi* conidiospore formation (fig. S3C inserts). Similar to interactions with *Bgh*, SAG101 and PAD4 exerted redundant functions against *E. pisi* colonization, and impairment of these two postinvasion resistance components alone was sufficient to allow occasional *E. pisi* sporulation (fig. S3C). Absence of PEN2 in a *pad4 sag101* background (*pen2 pad4 sag101* triple mutants) greatly enhanced disease susceptibility such that the timing and extent of *E. pisi* colonization became macroscopically indistinguishable from wild-type *Arabidopsis* interactions with the virulent *G. orontii* species (Fig. 3B and fig. S3D). Collectively, these findings strongly suggest separate functions for PEN2 in preinvasion and the EDS1-PAD4-SAG101 signaling complex in postinvasion nonhost resistance to both nonadapted powdery mildews.

The pathogen-triggered accumulation of PEN2-containing peroxisomes reported in this study (fig. S3A) as well as the recruitment of PEN1 syntaxin in a plasma membrane microdomain at fungal entry sites (*6*, *7*) are inconsistent with a preformed and passive barrier against fungal ingress, implying instead the existence of an inducible resistance mechanism at the cell periphery. We have shown here conserved PEN1 and PEN2 functions in preinvasion resistance to both tested nonadapted powdery mildew species that, together, explain almost all failed entry attempts (*pen1 pen2* double mutants) (Fig. 1). A corollary of this finding is that host powdery mildews such as *G. orontii* must have evolved means to overcome or bypass PEN activities. Two lines of evidence suggest that PEN1 and

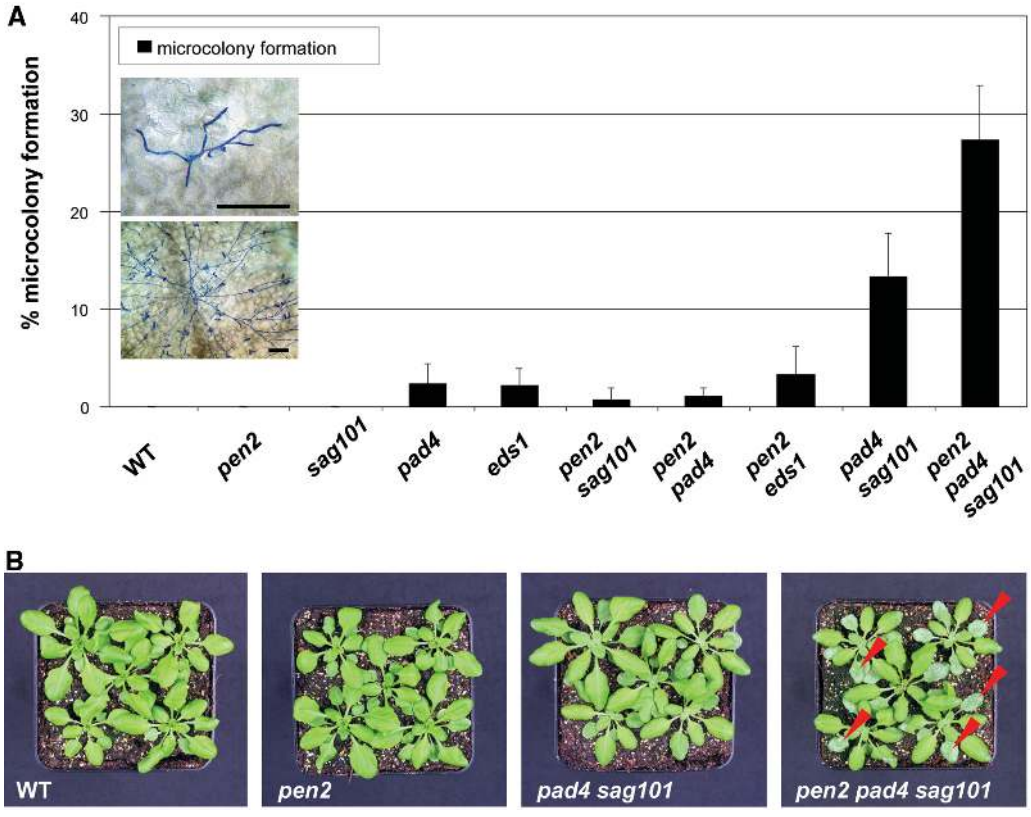

Fig. 3. Separable functions for PEN2 in preinvasion and the EDS1-PAD4-SAG101 signaling complex in postinvasion nonhost immunity. (**A**) Frequency of *Bgh* microcolonies on leaves of wild-type and mutant genotypes 7 days post–conidiospore inoculation (determined by calculating the incidence of microcolonies found per interaction site supporting epiphytic growth). The two light microscopic inserts show examples of a small (top) and a large (bottom) microcolony. The latter were only detectable on *pad4*-1 *sag101*-2 and *pen2*-1 *pad4*-1 *sag101*-2 lines. Error bars indicate standard deviations for triplicate measurements. (**B**) Macroscopic infection phenotypes of wild type and the indicated mutant genotypes 7 days post–*E. pisi* conidiospore inoculation. Red arrowheads denote leaves of *pen2*-1 *pad4*-1 *sag101*-2 plants that are densely covered by sporulating *E. pisi* fungal mycelium.

PEN2 represent components of two distinct entry resistance mechanisms: the broader spectrum of biological activity of PEN2 and the accumulative effect seen in *pen1 pen2* double null mutants in interactions with *Bgh*. Thus, we consider a simple model in which cargo of PEN2-containing peroxisomes is secreted via a putative PEN1 ternary SNARE complex unlikely. Failure of the $PEN2_{E183D}$ variant to complement the *pen2* mutant phenotype indicates that catalytic activity is required for PEN2 function. This makes it unlikely that PEN2 acts indirectly through interactions with other proteins. However, the peroxisomal localization and focal accumulation of PEN2 at fungal entry sites suggests that subcellular localization is an additional determinant for PEN2 function. The congregation of PEN2-containing peroxisomes at fungal entry sites might provide a mechanism for the activation and release of a small molecule at a high concentration. Because PEN2 inhibits *in planta* the pathogenesis of diverse fungal parasites, its catalytic product might directly or indirectly exert broad-spectrum toxic activity. Irrespective of this, our findings reveal a link between immune responses and a genetically defined peroxisomal component. Conceptually, the proposed pathogen-triggered focal secretory process, including PEN1 syntaxin and concentration of PEN2 F1GH at fungal entry sites, is reminiscent of the polar secretion machinery in cytotoxic T cells that is induced upon T cell receptor recognition, leading to targeted release of lytic proteins and killing of target cells (*14*).

Although previous reports demonstrated the involvement of lipase-like EDS1 in nonhost resistance to the grass powdery mildew fungus (*15*, *16*), we have shown here that the combined PAD4 and SAG101 contributions to postinvasion nonhost resistance greatly exceed those of the single components EDS1, PAD4, or SAG101. Our findings of redundant PAD4 and SAG101 activities in nonhost resistance are reminiscent of recently reported redundant PAD4 and SAG101 signaling functions in basal and R protein–triggered immunity (*13*), thereby pointing to the involvement of plant immune receptors in triggering nonhost resistance. One possible receptor class that could operate in nonhost resistance and act via PAD4 and SAG101 signaling would be the PAMP receptors recognizing conserved pathogen-associated molecular patterns (*17*). Consistent with this, flagellin perception by the FLS2 receptor-like kinase leads to rapid transcriptional activation of *EDS1*, *PAD4*, and *SAG101* as well as *PEN1*, *PEN2*, and *PEN3* (*18*). Thus, it is possible that pre- and postinvasion nonhost resistance components represent two branch pathways activated by the same immune receptors or are components of two pathways that are sequentially activated by different receptors. One potential advantage of the inferred two-layer concept for nonhost resistance to powdery mildews is robustness through functional redundancy, because pre- and postinvasive immune responses are each sufficient to terminate fungal pathogenesis.

References and Notes

1. J. Mengaud, H. Ohayon, P. Gounon, R. M. Mege, P. Cossart, *Cell* **84**, 923 (1996).
2. R. Panstruga, P. Schulze-Lefert, *Microbes Infect.* **5**, 429 (2003).
3. L. E. B. Johnson, W. R. Bushnell, R. J. Zeyen, *Can. J. Bot.* **60**, 1068 (1982).
4. D. G. Mellersh, I. V. Foulds, V. J. Higgins, M. C. Heath, *Plant J.* **29**, 257 (2002).
5. N. C. Collins *et al.*, *Nature* **425**, 973 (2003).
6. F. F. Assaad *et al.*, *Mol. Biol. Cell* **15**, 5118 (2004).
7. R. A. Bhat, M. Miklis, E. Schmelzer, P. Schulze-Lefert, R. Panstruga, *Proc. Natl. Acad. Sci. U.S.A.* **102**, 3135 (2005).
8. J. S. Bonifacino, B. S. Glick, *Cell* **116**, 153 (2004).
9. G. S. Saenz, J. W. Taylor, *Can. J. Bot.* **77**, 150 (1999).
10. Z. Xu *et al.*, *Plant Mol. Biol.* **55**, 343 (2004).
11. M. Czjzek *et al.*, *Proc. Natl. Acad. Sci. U.S.A.* **97**, 13555 (2000).
12. K. Nakai, P. Horton, *Trends Biochem. Sci.* **24**, 34 (1999).
13. B. J. Feys *et al.*, *Plant Cell* **17**, 2601 (2005).
14. G. Bossi, G. M. Griffiths, *Semin. Immunol.* **17**, 87 (2005).
15. B. W. Yun *et al.*, *Plant J.* **34**, 768 (2003).
16. L. Zimmerli, M. Stein, V. Lipka, P. Schulze-Lefert, S. Somerville, *Plant J.* **40**, 633 (2004).
17. C. Zipfel, G. Felix, *Curr. Opin. Plant Biol.* **8**, 353 (2005).
18. C. Zipfel *et al.*, *Nature* **428**, 764 (2004).
19. We thank H. Häweker and B. Pickel for excellent technical assistance, B. Weisshaar for providing *PEN2* T-DNA insertion line *pen2*-2 (GABI-KAT 134C04), and I. Somssich for critical reading of the manuscript. This work was supported by the GABI-NONHOST consortium funded by Bundesministerium für Bildung und Forschung and BASF Plant Science. A.M. was funded by the Ministerio de Educacion y Ciencia, Spain (grant BIO2003-4424).

Supporting Online Material
www.sciencemag.org/cgi/content/full/310/5751/1180/DC1
Materials and Methods
Figs. S1 to S3

26 August 2005; accepted 18 October 2005
10.1126/science.1119409